

Theory of the elasticity of nanometer-sized objects

D.E. Segall*, Sohrab Ismail-Beigi* & T.A. Arias†

*Department of Physics, Massachusetts Institute of Technology, Cambridge, Massachusetts 02139, USA

†Department of Physics, Cornell University, Ithaca, New York 14853, USA

DRAFT DATE: December 2, 2024.

Submitted to *Nature*

The recent development of artificial free-standing structures of nanometer dimensions opens a new series of fundamental questions about elasticity on scales where matter can no longer be viewed as a continuum. A wealth of experimental information is now available on the mechanics of nanowires and nanotubes[1, 2, 3, 4, 5, 6], and a computational literature is developing on the subject[7, 8, 9, 10, 11, 12, 13]. Many of these works, without formal justification, make use of results from continuum elasticity theory to analyze the behavior of nanometer structures. It is not yet known to what extent and in what ways relations from continuum elasticity theory break down on the nanoscale. It is also unclear what rigorous theory can stand as an intermediary between *macroscopic* elasticity and *microscopic* lattice dynamics. Here, we formulate a rigorous theory of elastic response on the nanoscale based upon physical observables. This theory gives the first *local* atomic-level analysis of elastic response in nanostructures and, therefore, allows quantitative understanding of how continuum theory breaks down on the nanoscale, how to make appropriate corrections, and how to predict the effects of different bonding arrangements on overall elastic response.

As an application, we show that this analysis leads to a new relation between the bending and stretching properties of nanomechanical resonators which is much more accurate than the continuum-based relations currently employed in experimental analyses.

In nanoscale objects, the inter-atomic spacing is no longer much smaller than the cross-sectional diameter, and care must be taken to define elastic constants properly. For long, thin resonators whose length greatly exceeds the inter-atomic spacing (Fig. 1), the resonator may be properly coarse-grained as a *one-dimensional* con-

tinuum. To lowest order, the free energy per unit length is then $f = (Eu^2 + Fr^{-2} + Tt^2)/2$, where u , r and t are the linear strain of extension, the radius of curvature of flexion and the rate of twist of torsion, respectively, and the coupling constants E , F and T are the *extensional rigidity*, the *flexural rigidity* and the *torsional rigidity*, respectively. This free-energy function is experimentally observable in principle and thus provides an unambiguous operational definition of the rigidities.

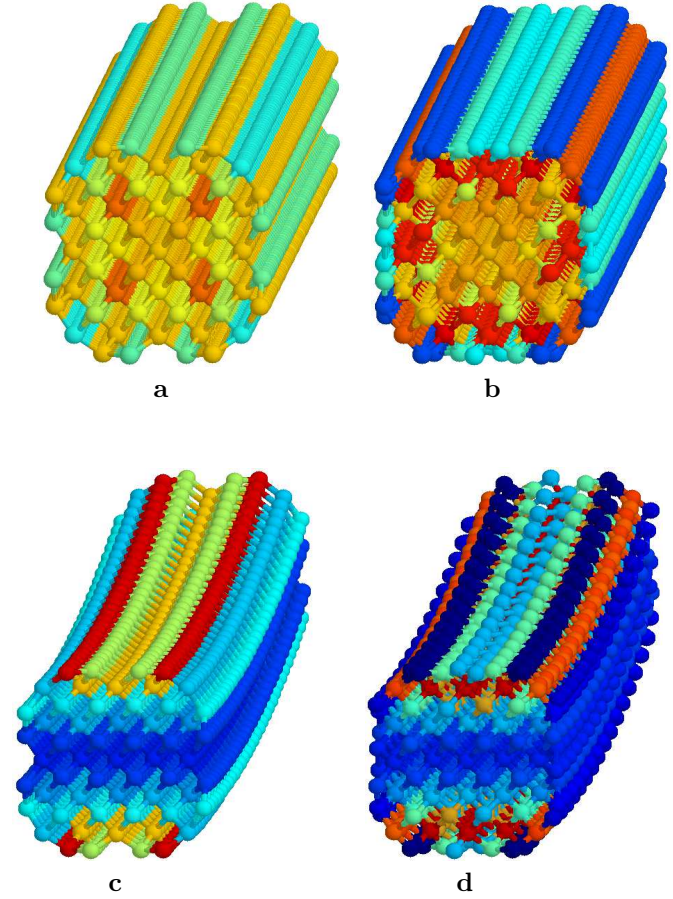


FIG. 1: Atomic structure of silicon nanowires of 1.5 nm cross-sectional diameter viewed along the longitudinal axis when under extension (a,b) or flexion (c,d) for the “ $c(2 \times 2)$ ” structure (a,c) and the “ 2×1 ” structure (b,d). Colors (blue to red) indicate atomic contributions (small to large, respectively) to the corresponding rigidities: equation 12 for extension (a,b) and equation 4 for flexion (c,d). The figure underscores the impact of different local environments on the atomic moduli, and the emphasis which flexion, as opposed to extension, places the surfaces.

The Methods Section develops the relationship between long-wavelength lattice dynamics and elasticity theory to provide an exact decomposition of the extensional rigidity E into a sum over individual atomic con-

tributions e_α (equation 11). The straightforward, naïve analysis of the sum in equation 11 assigns as the contribution from a given atom the sum of all terms which refer to it. Mathematically, this corresponds to equation 13 with the terms as defined in equation 14. We refer the reader to the Methods Section for precise definitions of all mathematical quantities to which we refer below.

Other such decompositions into “atomic level moduli” either have not accounted for internal relaxations such as the Poisson effect, and thus do not sum to the overall response for nanoscale systems, or ascribe arbitrary, physically unobservable energies to individual atoms[14, 15]. These alternate decompositions correspond closely to the aforementioned straightforward analysis of equation 11 and exhibit the same failures in nanoscale systems described shortly below. In particular, for nanoscale systems, they do not analyze elastic response into contributions which depend only on the local atomic environment, they lead to moduli which scale linearly with the size of the system for the atoms at the surfaces, and they result in predictions for flexural properties which are less accurate than those of the straightforward continuum theory.

Analyses which correspond to equation 11 are useful primarily for the study of infinite bulk systems. For such systems, elastic waves are planar, so that the first-order polarization vector ($\vec{u}_\alpha^{[1]}$) is uniform from primitive cell to primitive cell and thus dependent only upon the local environment of each atom. Although the strain terms ($\Delta\vec{r}_{\alpha\beta}$) scale linearly with distance between atoms and therefore have the potential to scale with the size of the system, these terms always appear in products with the force-constant matrix ($\Phi(\vec{R})$). The magnitude of the strain terms which actually contribute to the final result is therefore bounded by the range of the interatomic interactions. These considerations ensure that each atomic modulus (e_α) depends only upon the *microscopic* environment of the corresponding atom and not on the *macroscopic* size of the system.

Such decomposition into locally dependent contributions becomes critical as systems approach the nanoscale, where continuum descriptions break down and where mechanical response becomes sensitive to rearrangements in local bonding such as surface reconstructions. However, as Figure 2a shows, for nanoresonators the above naïve analysis results in surface moduli which scale with the size of the resonator and thus fail to depend solely on the local atomic environment. Below, we show that, as a consequence of this behavior, such moduli are of little use in understanding flexural properties from first principles.

This failure arises ultimately from the fact that elastic waves in nanoresonators (or any nanoscale system with free surfaces) are not strictly planar, but rather involve extensive displacements. In particular, the Poisson effect, which the first-order polarization vector ($\mathbf{u}^{[1]}$) describes, causes each atom to displace by an amount in direct proportion to its distance from the center line of the system and leads to the linear scaling of the atomic moduli

at the surfaces observed in Figure 2a. A distinguishing characteristic of systems with free surfaces is that that the local distortions involved with long-wavelength acoustic modes can involve not only translations but also rotations. Explicit use of the corresponding continuous symmetries allow us to recast the atomic moduli into a local form which does not exhibit the linear scaling in Figure 2a.

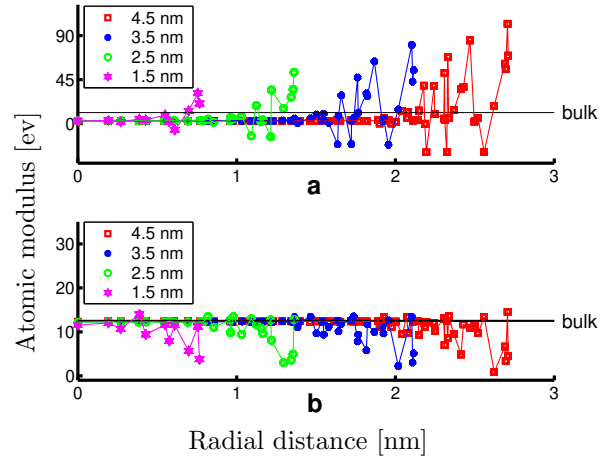


FIG. 2: Atomic moduli as a function of radial distance for $c(2 \times 2)$ nanoresonators of varying cross-sectional diameter (1.5, 2.5, 3.5 and 4.5 nm): (a) naïve and (b) nanoscopic analyses. Panel (a) demonstrates that, on the surfaces of the resonators, the naïvely defined moduli diverge with the diameter of the resonator and thus become of little use in understanding the mechanical properties of the surface. Moreover, in the interior these moduli fail to approach the expected bulk value $e_b \equiv Y_b/\rho_b$, where Y_b and ρ_b are the Young’s modulus and number density of bulk, respectively. Panel (b) shows that the newly developed nanoscopic analysis does not suffer these defects and indeed resolves overall response into local contributions.

To separate extensive elastic effects from intensive nanoscopic motions we first redefine the atomic displacements ($\vec{u}_\alpha^{r,l}$) as the intensive nanoscopic motions which occur in addition to the extensive Poisson motion,

$$\vec{u}_\alpha^{r,l} \equiv \vec{u}_\alpha^{[1]} - ((-\sigma_x \hat{x}\hat{x} \cdot -\sigma_y \hat{y}\hat{y} \cdot) \vec{r}_\alpha), \quad (1)$$

where the σ are the bulk Poisson ratios. The continuous rotational and the translational symmetries of the dynamical matrix then allow us, after some algebra, to generate a local analysis of the elastic response which retains the form of equation 13 but with $\Delta\vec{r}_{\alpha\beta}$ redefined and $\Psi_{\alpha\beta}(\vec{R})$ renormalized,

$$\Delta\vec{r}_{\alpha\beta} \equiv (\hat{z}\hat{z} \cdot -\sigma_x \hat{x}\hat{x} \cdot -\sigma_y \hat{y}\hat{y} \cdot) (\vec{r}_\alpha - \vec{r}_\beta - \vec{R}), \quad (2)$$

$$\Psi_{\alpha\beta}(\vec{R}) \equiv 2\Phi_{\alpha\beta}(\vec{R}) - \left(\text{Tr} \Phi_{\alpha\beta}(\vec{R}) \cdot \Sigma \right) \Sigma^{-1}. \quad (3)$$

Here, $\Sigma_{jk} \equiv \delta_{jk}\sigma_j$ is a diagonal 3×3 matrix with non-zero elements $\sigma_{x,y,z}$, where $\sigma_z \equiv -1$. Now, $\Delta\vec{r}_{\alpha\beta}$ represents

the total elastic strain between atoms α and β , including the Poisson effect, and $\Psi_{\alpha\beta}(\vec{R})$ is the corresponding, renormalized force-constant matrix.

It is now the range of the force-constant matrix which controls the size of the neighborhood upon which each atomic modulus depends. This is because \vec{u}_α^l no longer includes extensive motions, while $\Delta\vec{r}_{\alpha\beta}$ still depends only upon relative atomic distances and the renormalized Ψ still decays as does Φ . This new construction now ensures that the modulus of each atom depends only upon its local atomic environment. The moduli of atoms in the interior now *must* correspond to the expected bulk value and the moduli of the atoms on the surface now *cannot* depend upon the extent of the system. Figure 2b illustrates the success of the new, nanoscopic analysis. Note that the rapid approach to the bulk value while moving inward from the surface provides a clear prescription for defining the mechanical depth of the surface from first principles. Finally, Figure 1(a,b) shows the dependence of the new moduli on atomic environment and serves to illustrate the role of surface reconstruction in local elastic response.

To demonstrate that our atomic moduli indeed characterize the physics of elasticity at the atomic scale, we now show that they are transferable to phenomena not considered in their original construction. In flexion, for example, if the atomic moduli indeed describe the local response to strain, the free energy per unit length should take the form $f = (1/L_c) \sum_\alpha e_\alpha u_\alpha^2/2$, where u_α is a measure of the longitudinal strain which atom α experiences. For this form to be sensible, the range of the force-constant matrix must not become comparable to the cross-section of the wire, so as to ensure that the atoms which contribute to a specific e_α all experience similar strains (u_α). Within continuum theory, uniform flexion with radius of curvature r corresponds to a longitudinal strain which varies linearly across the wire ($u = x/r$), which we have verified to an accuracy of better than one part in 10^4 for the wires in this study. This gives an atomic-moduli prediction for the flexural rigidity of

$$F_{at} = \frac{1}{L_c} \sum_\alpha e_\alpha x_\alpha^2. \quad (4)$$

Fig. 3 shows that for all but the thinnest resonators the error associated with this prediction (as compared to direct computation) is far smaller than that of the standard continuum theory. The linear behavior of the fractional error δF_{cnt} with $1/D$ indicates that continuum theory does not properly account surface effects. This results from the fact that flexion places a larger emphasis on the surface than does extension, as Fig. 1 depicts. The dramatic improvement from use of equation 4 arises because the atomic moduli place proper emphasis on the surface and on the interior as they treat each atomic environment individually. The only appreciable error within the new framework occurs for the smallest wires with

1.5 nm diameter. At this point, a new length scale enters: the cross-sectional dimension becomes comparable to the range of the force-constant matrix, and the flexural rigidity now requires a full lattice-dynamics analysis.

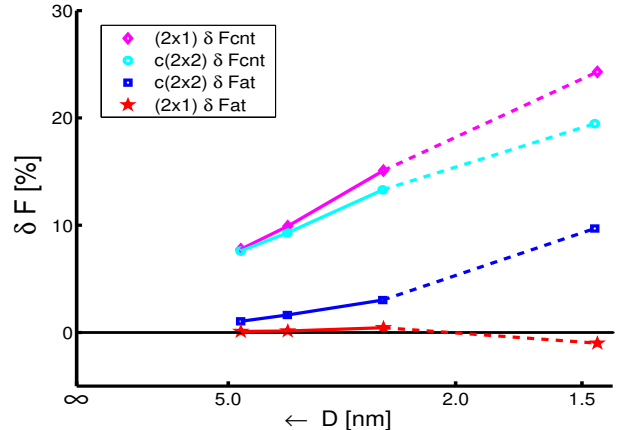


FIG. 3: Fractional error in percent of the prediction of flexural rigidity from within the atomic moduli approach (δF_{at}) and standard continuum theory (δF_{cnt}). Note that $F_{cnt} = E(I/A)$, where I is the moment of inertia of the cross-section and A is the corresponding area. Although A is not well-defined on the nanoscale, for the purpose of this plot, we interpret the ratio I/A as the (well-defined) mean moment of inertia per unit length, $I/A = (1/N_c) \sum_\alpha x_\alpha^2$. For these comparisons, we determine the exact rigidities directly from perturbation theory on the dynamical matrix. Also, we estimate the cross-sectional diameter of the resonators as $D \approx \sqrt{\lambda/\rho_b}$ where λ is the linear atomic number density of the resonator.

Another advantage of having a rigorously defined concept of atomic-level moduli which depend only upon the local environment is that it provides insight into the failures of standard continuum relations and leads to prescriptions for appropriate corrections. We now demonstrate this by predicting much more accurately than can standard continuum relations in current use, the extensional rigidity in terms of the directly measured flexural rigidity (in our case, computed directly) and other experimentally accessible quantities. This new relation is of interest because direct measurements of extensional properties are often very difficult on the nanoscale[1, 2, 5, 6].

Equations 4 and 12 predict the extensional modulus as

$$E_{at} = \frac{1}{2} \left(\frac{F}{I/A} + Y_b \frac{\lambda}{\rho_b} \right), \quad (5)$$

with higher-order corrections given *exactly* by $E \delta E_{at}^{(p)}$, where

$$\delta E_{at}^{(p)} = \frac{N_s}{EL_c} \{ B_{at} [\langle e_s \rangle_{x^2} - e_b] + [\langle e_s \rangle_{x^2} - \langle e_s \rangle] \}. \quad (6)$$

Here N_s is the number of “surface” atoms, those for which e_α differs significantly from e_b , $\langle e_s \rangle_{x^2} \equiv$

$(\sum_s e_s x_s^2)/(\sum_s x_s^2)$ and $\langle e_s \rangle \equiv (\sum_s e_s)/N_s$ with the sums ranging over “surface” atoms, and $B_{at} \equiv (1/2)\langle x_s^2 \rangle/\langle x_c^2 \rangle - 1$, where the subscripts s and c refer to unweighted averages over the surface and over the entire unit cell, respectively. This result holds for any division of the atoms into “surface” and “bulk” to the extent that each “bulk” atom has atomic modulus e_b and that equation 4 gives the flexural rigidity. Figure 4 shows that the new relation, equation 5, improves dramatically upon the continuum result.

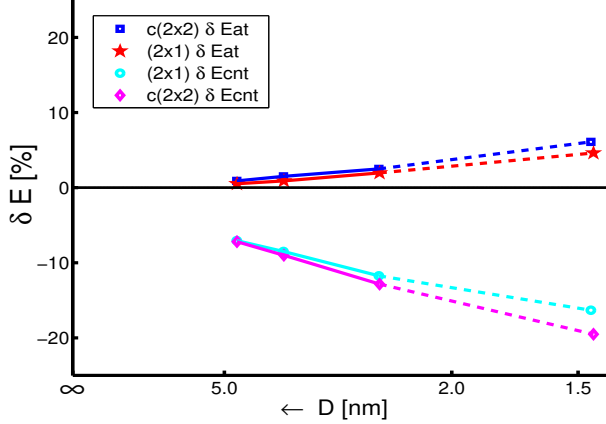


FIG. 4: Fractional error in predicting the extensional rigidity from flexural properties using either the new relation, equation 5 (δE_{at}), or the standard continuum relation, $E_{cnt} = F/(I/A)$ (δE_{cnt}). For these comparisons, we determine the exact rigidities directly from perturbation theory on the dynamical matrix. The figure shows that the standard continuum relation underestimates the extension rigidity by as much as 10–20% for wires with cross-sections of 1.5–5 nm, whereas the atomic-moduli based relation, equation 5, improves the prediction by over an order of magnitude for resonators of diameter greater than 2 nm. As in Fig. 3, the linear behavior of the error with $1/D$ indicates that the continuum prediction does not account surface effects properly.

From the atomic-moduli, we may understand in detail the origin of the great improvement of equation 5 over the traditional continuum relation. Equations 4 and 12 also yield a prediction for the fractional error in the continuum analysis,

$$\delta E_{cnt}^{(p)} = \frac{N_s}{EL_c} \{ B_{cnt} [\langle e_s \rangle_{x^2} - e_b] + [\langle e_s \rangle_{x^2} - \langle e_s \rangle] \}, \quad (7)$$

which takes precisely the same form as equation 6, but with $B_{cnt} \equiv 2B_{at} + 1$ replacing B_{at} . We now note that the term in the first set of square brackets in equations 6 and 7, an average difference between surface and bulk atoms, is generally much larger than the term in the second set of square brackets, the difference between two differently weighted averages over the surface atoms. For wires of homogeneous cross-section with circular or regular polygonal shapes, we have that $B_{at} = 0$ and $B_{cnt} = 1$.

Thus, when using the new relation (equation 5), the first, larger term in $\delta E_{at}^{(p)}$ nearly vanishes, while for the standard continuum relation this larger term remains and contributes to much larger errors.

Finally, equation 7 shows that the naïve definitions of the atomic moduli give an incorrect description of flexion. In the continuum limit, the quantity defined as $\delta E_{cnt} = (F/(I/A) - E)/E$ in Figure 4 in terms of the true rigidities of the resonator E and F must approach zero. Equation 7 gives this quantity in terms of the physical value of E and the value of F predicted from the atomic moduli (equation 4). Note that the prefactor in equation 7, $N_s/(EL_c)$, scales as $1/D$ where D is the diameter of the resonator. If, now, one predicts F using naïvely defined moduli which scale as D on the surface as in Figure 2a, then $\delta E_{cnt}^{(p)}$ does not approach zero, but rather a constant. This implies that equation 4 makes an error which scales as $E(I/A) \sim D^4$, more severely than even the surface corrections to continuum theory. On the other hand, with a properly local definition, the surface moduli remain finite, $\delta E_{cnt}^{(p)}$ approaches zero, and equation 4 gives a proper description of flexion.

To conclude, this letter presents the first atomic-level elastic moduli for nanoscale systems which are defined in terms of physical observables, sum to give the exact collective elastic response, depend only on the local atomic environment, and transfer among different modes of strain. This new concept leads to a new and much more accurate method for relating extensional and flexural rigidities in terms of experimental observables, allows the identification of which atomic arrangements lead to more pliant or stiffer response, provides a clear and natural method for distinguishing *mechanically* between “surface” atoms and “bulk” atoms, and opens the opportunity to understand the relation between mechanical response and the underlying electronic structure. In addition, this new definition has the practical advantage that it may be applied in conjunction with any technique which yields the dynamical matrix, including empirical potentials, tight binding models, and *ab initio* methods. □

Methods

Physical models, coordinates, and definitions

For concreteness, here and in the above analyses, we consider the behavior of (100)-oriented nanoresonators of silicon, which recent *ab initio* studies predict to undergo a size-dependent structural phase transition at cross-sectional diameters of about ~ 3 nm between the $c(2 \times 2)$ structure and the 2×1 structure[16]. (See Figs. 1(a,b).) In this work, we employ the Stillinger-Weber interatomic potential[17], which gives a sufficiently accurate and efficient description for silicon for our present purpose of exploring general nanoelastic phenomena in unit cells with thousands of atoms.

We choose coordinates such that the origin lies on the center line of each resonator, which we take to run along the z -axis. We then orient the remaining coordinate axes so that the transverse symmetry planes of each resonator are perpendicular to the x and

y -axes. Here, unlike in the bulk crystal, the primitive unit cell includes the entire cross-section of the wire and thus many atoms. We denote the number of atoms in this cross-sectional unit cell by N_c , its length by L_c , and the linear atomic number density of the resonator by $\lambda = N_c/L_c$. The atomic number density of bulk we denote ρ_b . In our equations, we use boldfaced quantities represent $3N_c$ -dimensional quantities, arrowed vectors for three-dimensional quantities, and Greek indices to range over all atoms in the unit cell. Finally, to characterize elastic response, we define Y_b as the bulk Young's modulus and σ_x and σ_y as the Poisson ratios of the bulk material. Whenever numerical values are needed for these parameters, we employ the corresponding values of the Stillinger-Weber model.

Continuum theory and lattice dynamics

Continuum theory predicts the longitudinal and transverse acoustic dispersion relations to be connected to the elastic rigidities E and F through

$$\begin{aligned}\omega_{LA} &= \sqrt{E/(\lambda m)}q \\ \omega_{TA} &= \sqrt{F/(\lambda m)}q^2,\end{aligned}\quad (8)$$

where ω is the frequency, q is the wave vector and m is the atomic mass (assumed constant for simplicity).

Born and Huang developed, for *macroscopic* systems, the connections between continuum elasticity theory and the theory of lattice dynamics through their "method of long waves"[18], which coarse grains away all length scales smaller than the continuum. Beginning similarly, we define the Bloch phase such that it varies linearly along z , thus ensuring a uniform description of the distribution of elastic energy along the unit cell. To generate a scalar equation for the phonon frequency, Born and Huang project the secular equation for the dynamical matrix $\mathbf{D}\mathbf{u} = -m\omega^2\mathbf{u}$ against the zeroth-order polarization vector $\mathbf{u}^{[0]}$. Here, however, to more symmetrically represent the distribution of elastic energy, we project against the full polarization vector \mathbf{u} .

Equating the frequency ω which results from this projection of the secular equation with the longitudinal frequency in equation 8 creates the connection between the dynamics of the lattice and the extensional rigidity,

$$-\frac{E}{\lambda} = \frac{[\mathbf{u}^\dagger \mathbf{D} \mathbf{u}]^{[2]}}{\mathbf{u}^\dagger \mathbf{u}} = \sum_{s,t=0}^1 \frac{(-1)^s}{N_c} \mathbf{u}^{\dagger[s]} \mathbf{D}^{[2-s-t]} \mathbf{u}^{[t]}.\quad (9)$$

Here, the superscripts indicate powers of (iq) in the perturbation expansion for small wave-vectors q , and the 3×3 sub-block of $\mathbf{D}^{[n]}$ which couples atoms α and β is

$$[\mathbf{D}^{[n]}]_{\alpha\beta} = \frac{1}{n!} \sum_{\vec{R}} \Phi_{\alpha\beta}(\vec{R}) \left(\hat{z} \cdot (\vec{R} + \vec{\tau}_\beta - \vec{\tau}_\alpha) \right)^n,\quad (10)$$

where $\Phi_{\alpha\beta}(\vec{R})$ is the sub-block of the force-constant matrix coupling atoms α and β in unit cells $\vec{0}$ and \vec{R} , respectively, and $\vec{\tau}_\alpha$ and $\vec{\tau}_\beta$ are the basis vectors of the corresponding atoms.

To analyze the extensional rigidity E in terms of the underlying physics, we substitute equation 10 and $[\mathbf{u}^{[0]}]_\alpha = \hat{z}$ into equation 9, which leads to

$$E = \frac{1}{L_c} \sum_{\alpha} \sum_{\beta} \sum_{s,t=0}^1 (-1)^{(s+1)} \bar{u}_\alpha^{\dagger[s]} \cdot \mathbf{D}_{\alpha\beta}^{[2-s-t]} \cdot \bar{u}_\beta^{[t]}\quad (11)$$

$$= \frac{1}{L_c} \sum_{\alpha} e_\alpha\quad (12)$$

$$\begin{aligned}e_\alpha \equiv \sum_{\beta \vec{R}} \left\{ -\Delta \vec{r}_{\alpha\beta} \cdot \Psi_{\alpha\beta}(\vec{R}) \cdot \Delta \vec{r}_{\alpha\beta} / 2 + \bar{u}_\alpha^{r_l} \cdot \Phi_{\alpha\beta}(\vec{R}) \cdot \bar{u}_\beta^{r_l} \right. \\ \left. + \Delta \vec{r}_{\alpha\beta} \cdot \Phi_{\alpha\beta}(\vec{R}) \cdot \bar{u}_\beta^{r_l} - \bar{u}_\alpha^{r_l} \cdot \Phi_{\alpha\beta}(\vec{R}) \cdot \Delta \vec{r}_{\alpha\beta} \right\},\end{aligned}\quad (13)$$

where we refer to the e_α as the "atomic moduli." The naïve, straightforward decomposition of equation 11 into equations 12 and 13 defines the three quantities $\bar{u}_\alpha^{r_l}$, $\Psi_{\alpha\beta}(\vec{R})$ and $\Delta \vec{r}_{\alpha\beta}$ as

$$\begin{aligned}\bar{u}_\alpha^{r_l} &\equiv \bar{u}_\alpha^{[1]} \\ \Psi_{\alpha\beta}(\vec{R}) &\equiv \Phi_{\alpha\beta}(\vec{R}) \\ \Delta \vec{r}_{\alpha\beta} &\equiv \hat{z} \hat{z} \cdot (\vec{\tau}_\alpha - \vec{\tau}_\beta - \vec{R})\end{aligned}\quad (14)$$

This letter demonstrates that this naïve decomposition fails for nanoscale systems and develops, for such systems, the first appropriate decomposition in terms of well-defined physical observables.

-
1. Wong, E. W., Sheehan, P. E. & Lieber, C. M. Nanobeam mechanics: elasticity, strength, and toughness of nanorods and nanotubes. *Science* **277**, 1971-1975 (1997).
 2. Osakabe, N., Harada, K., Lutwyche, M. I., Kasai, H. & Tonomura, A. Time-resolved observation of thermal oscillations by transmission electron microscopy. *Appl. Phys. Lett.* **70**, 940-942 (1997).
 3. Cleland, A. N. & Roukes, M. L. Fabrication of high frequency nanometer scale mechanical resonators from bulk Si substrates. *Appl. Phys. Lett.* **69**, 2653-2655 (1996).
 4. Carr, D. W. & Craighead, H. G. Fabrication of nanoelectromechanical systems in single crystal silicon using SOI substrates and electron beam lithography. *J. Vac. Sci. Technol. B* **15**, 2760-2763 (1997).
 5. Treacy, M. M. J., Ebbesen, T. W. & Gibson, J. M. Exceptionally high Young's modulus observed for individual carbon nanotubes. *Nature* **381**, 678-680 (1996).
 6. Salvetat, J. P., *et al.* Elastic and shear moduli of single-walled carbon nanotube ropes. *Phys. Rev. Lett.* **82**, 944-947 (1999).
 7. Hernández, E., Goze, C., Bernier, P. & Rubio, A. Elastic Properties of C and B_xC_yN_z composite nanotubes. *Phys. Rev. Lett.* **80**, 4502-4505 (1998).
 8. Yakobson, B. I., Brabec, C. J. & Bernholc, J. Nanomechanics of carbon tubes: instabilities beyond linear response. *Phys. Rev. Lett.* **76**, 2511-2514 (1996).
 9. Robertson, D. H., Brenner, D. W. & Mintmire, J. W. Energetics of nanoscale graphitic tubules. *Phys. Rev. B* **45**, 12592-12595 (1992).
 10. Lu, J. P. Elastic properties of carbon nanotubes and nanoropes. *Phys. Rev. Lett.* **79**, 1297-1300 (1997).
 11. Mon, K. K. Mechanical properties of model nanostructures. *Phys. Rev. B* **50**, 16718-16721 (1994).
 12. Mon, K. K. Size dependence of model nanostructure sound velocity. *J. Appl. Phys.* **80**, 2739-2741 (1996).
 13. Cornwell, C. F. & Wille, L. T. Elastic properties of single-walled carbon nanotubes in compression. *Solid State Commun.* **101**, 555-558 (1997).
 14. Shibutani, Y., Vitek, V. & Bassani, J. L. Nonlocal properties of inhomogeneous structures by linking approach of generalized continuum to atomistic model. *Int. J. Mech. Sci.* **40**, 129-137 (1998).
 15. Alber, I., Bassani, J. L., Khantha, M., Vitek, V. & Wang G. L. Grain boundaries as heterogeneous systems: atomic and continuum elastic properties. *Phil. Trans. R. Soc. Lond. A* **339**, 555-586 (1992).
 16. Ismail-Beigi, S. & Arias, T. Edge-driven transition in the surface structure of nanoscale silicon. *Phys. Rev. B* **57**, 11923-11926 (1998).
 17. Stillinger, F. H. & Weber, T. A. Computer simulation of local order in condensed phases of silicon. *Phys. Rev. B* **31**, 5262-5270 (1985).
 18. Born, M. & Huang, K. in *Dynamical Theory of Crystal Lattices*. (Oxford University Press, London, 1954).

Acknowledgements

Computational support was provided by the MIT Xolas prototype SUN cluster, and the Cornell Center for Materials Research Shared Experimental Facilities, supported through the NSF MRSEC program. D.E. Segall acknowledges support of a fellowship from the MIT Department of Physics and the continuing support of the department, and Sohrab Ismail-Beigi acknowledges support through the US DOE ASCI ASAP program.

Correspondence and requests for materials should be addressed to D.E.S.

(e-mail: desegall@mit.edu).